

DIGITAL HOLOGRAM DENOISING BY FILTERING IN THE HOLOGRAM PLANE USING THE HILBERT-HUANG TRANSFORM

SIMEON KARPUZOV, ASSEN SHULEV AND GEORGE PETKOV

Image quality degradation is one of the main problems in Digital Holography. A novel method for noise reduction based on the Hilbert-Huang transform is introduced that reduces the normalized contrast and partially removes the DC-term. It is successfully applied in the hologram plane and requires a single hologram to function. The method causes no reduction in spatial resolution. Moreover, it can be combined with existing noise-filtering methods to improve image quality even further.

Keywords: digital holography, noise filtering, Hilbert-Huang transform, empirical mode decomposition, scattered data interpolation

2020 Mathematics Subject Classification: 68U10, 68W01

CCS Concepts:

- Applied Computing~Physical sciences and engineering~Physics

1. INTRODUCTION

Digital holography is an optical technique used to capture and display information on both light intensity and phase [16,28]. It has applications in many different fields, such as microscopy [14,33], cryptography [6], nondestructive testing [9,12], art and entertainment displays [35] and others [15,31]. The technique uses lasers as a light source, and due to their coherent nature, digital holograms exhibit a mixture of highly coherent speckles and additive incoherent noise. These effects severely degrade the quality of the recorded holograms, and significant effort is put into limiting the noise.

Generally speaking, two main classes of techniques tackle the hologram noise problem: optical and numerical. Optical methods involve some reconfiguration of the

standard recording holographic setups, such as multiple wavelength recording [13], white-light illumination [24], moving diffusers and apertures [17] and others [23]. They all show substantial noise reduction qualities, and some of the best available methods are part of this class. Still, additional work and optical elements must be introduced during the digital hologram’s recording stage to benefit from them. The second group of methods, the numerical ones, utilizes standard holographic setups but processes numerically the recorded or reconstructed holograms. When operating on the recorded hologram, usually the goal is to produce multiple holograms in which the speckle patterns are de-correlated – the multi-look digital holography approach (MLDH). The best of these methods is demonstrated in [2]. The techniques that operate on the reconstructed image are various spatial filters, the best performing of which is BM3D [3, 4, 8]. Methods based on deep learning techniques also show promise, but they will not explore them here due to some practical considerations such as ease of applicability and result interpretability (especially for medical tasks) [36].

An area of digital hologram denoising left somewhat unexplored is filtering in the hologram plane without relying on the MLDH methods. This paper proposes a technique based on the Hilbert-Huang transform (HHT) [15] for two-dimensional data. The technique uses a single shot and a standard off-axis recording hologram setup. It is different from existing methods in the following two ways:

- The HHT is a global transformation method that works with the entirety of the signal.
- The method works with the recorded hologram, and the noise filtering occurs in the hologram plane.

The 2D-HHT technique can decompose the input hologram into several components, the sum of which is the original hologram. We hypothesize that some components are non-informative and only introduce noise or other unneeded low-frequency data. Such components can be discarded. The interaction between different components is going to be examined. We will omit and add new elements. Various combinations will be tested to find the best. When talking about a “*best one*”, it is strictly meant in the conditions of the current experiment with its specific parameters.

2. METHODS

The Hilbert-Huang transform is a novel way to decompose a signal into a data-dependent basis through the Empirical Mode Decomposition (EMD) [22] and obtain frequency information by using Hilbert Spectral analysis [19]. HHT works very well on nonstationary and nonlinear signals. This can be utilized in digital holography. The EMD process can be broken down into several steps:

1. Firstly, the local minima and maxima of the input signal $H_{i-1}(x, y)$ are identified;

2. Afterwards, cubic splines are used to connect those extrema, thus forming an upper and lower envelope – $E_u(x, y)$ and $E_l(x, y)$;
3. The mean of the two envelopes – $m(x, y) = \frac{1}{2}[E_u(x, y) + E_l(x, y)]$ is then subtracted from the original signal $H_i(x, y) = H_{i-1}(x, y) - m(x, y)$;
4. The process is repeated with the updated value $H_i(x, y)$ until an intrinsic mode function (IMF) with specific properties is found. Similarly to the one-dimensional case, the mean of the two envelope surfaces is zero and the number of local minima and maxima is approximately the same.
5. With the acquired IMF, steps 1–4 are repeated. The collection of IMFs represents the original data, and their sum is the starting signal – $H(x, y) = \sum_{i=1}^C \text{IMF}_i(x, y) + r_c$, where r_c is the signal trend, and C is the total number of IMFs.

After the EMD components have been obtained, frequency analysis can be performed by applying the Hilbert transform to each IMF. Depending on the task, various manipulations and processing can be used for single or multiple components, and components may be dropped or added from the collection of IMFs.

The original method applies to 1D data, but since its introduction, many authors have shown the possibility of extending the ideas to 2D signals [21, 27]. Some take shortcuts regarding interpolation or extrema localization, but we have attempted to stay true to the original technique. The recorded hologram is the 2D data on which we apply the HHT method. Since the data is two-dimensional, upper and lower envelope surfaces are built correspondingly through the local maxima and minima. The mean surface between the upper and lower envelope surfaces is subtracted from the original hologram, and the process continues until a singular frequency component remains. Building the envelope surfaces is a scattered data interpolation problem for which several algorithms have been developed [1, 10]. In the current work, the primary interpolating method is the biharmonic spline [26]. It is combined with a 2D cubic interpolating technique using Delaunay triangulation [20]. We usually calculate the first three to four components with the latter and then finish with the former algorithm. The reason for this approach is that for large data sets, the biharmonic spline requires a large amount of memory – 83 GB for 8 Mpix holograms. Using only cubic interpolation with triangulation also leads to convergence, but more components are generated and have significant amplitude differences. Other methods [25, 29] were also considered. However, it was found that the combination of the methods mentioned above led to a very stable convergence to a single oscillatory IMF. The next part of this paper presents an investigation into the interpolation methods and convergence, as well as component selection.

3. EXPERIMENTAL AND METHOD SETUP

An Nd: YAG laser with a wavelength of 532 nm is used as a light source. The light sensor is a CMOS camera with a pixel size of $1.67 \times 1.67 \mu\text{m}^2$. The distance

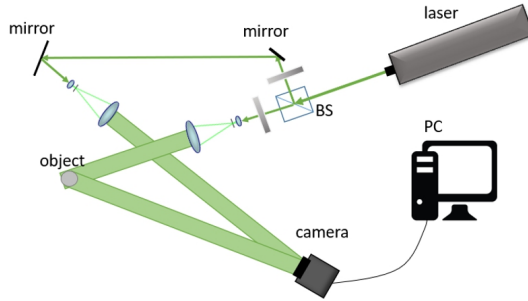


Figure 1. Standard off-axis holographic setup,
B.S. – beam splitter

between the object and the camera is 34 cm. The experimental setup used in the current work is shown in Figure 1.

In the current work, holograms were reconstructed using the Fresnel diffraction formula. Noise reduction is evaluated using the normalized contrast V , defined as

$$V = \frac{\sigma}{\mu}, \quad (3.1)$$

where σ and μ are the standard deviation and the mean of the pixel values of a homogenous area in the image. A lower value of the normalized contrast indicates less noise. Whenever “ground truth” information is available (as is in the case with computer generated holograms) mean squared error (MSE) can be used:

$$\text{MSE} = \frac{\sum_{m,n=1}^{M,N} (I_{\text{true}}(m,n) - I_{\text{noisy}}(m,n))^2}{M \times N} \quad (3.2)$$

where I_{true} is the ground truth image, I_{noisy} is the noisy image, $M \times N$ is their size.

The first step in preparing the algorithm that processes the holograms is to achieve convergence of the EMD stage. It is a challenging task as the local extrema are distributed in a non-structured manner throughout the two-dimensional image array (the recorded hologram). Our initial interpolating attempt was trying out the cubic interpolation based on Delaunay triangulation. This technique creates a piecewise $C1$ surface of the input scattered data. While the method is fast and could achieve convergence, it is not systematic and often produced over 25 components. This uncertain behaviour is unwanted. Purely linear interpolation and others, such as nearest and natural neighbour interpolation, do not achieve convergence. Those methods are also quite different from the spline interpolation used in the 1D case of Huang’s original work. Biharmonic splines were also tried out, but due to the high number of extrema ($> 4E+04$), they turned out to be very computationally and memory expensive. Due to this limitation, the biharmonic spline interpolation technique was chosen only for smaller holograms or EMD components with fewer local extrema ($< 4E+04$). For smaller holograms, the method is relatively stable and robust. Shepard’s interpolation method was also employed, but it achieved convergence slower than the biharmonic splines. The best result regarding systematic

convergence and the number of produced components was achieved using a combination of cubic interpolation and biharmonic splines. The cubic interpolation algorithm calculates the first three or four components as they are the most computationally intensive. After that, biharmonic splines are used. It solves the problems with convergence in the first method and the computational costs of the second. With this combination, we can achieve hologram convergence in 8 or 9 steps (depending on the hologram). An example decomposition using this approach is presented in Figure 2.

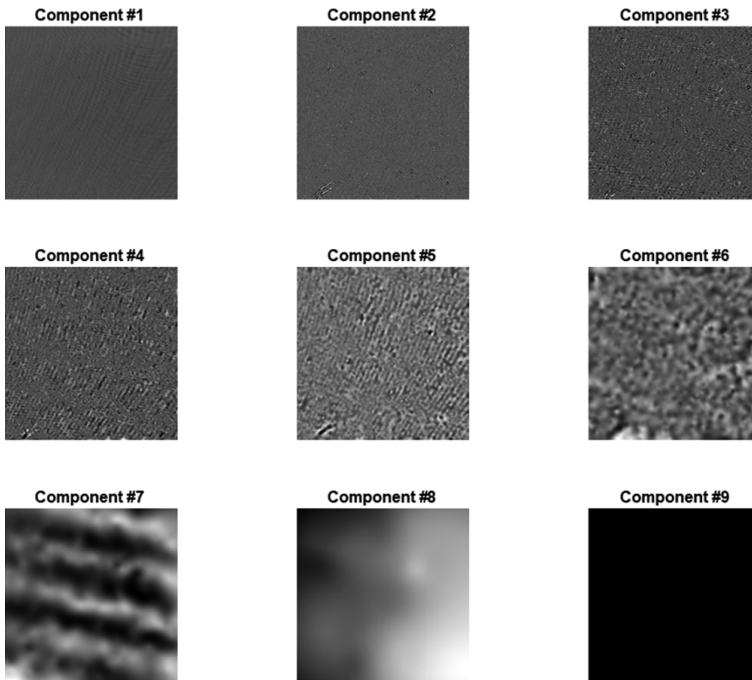


Figure 2. Decomposition of a hologram into 9 EMD components

Processing times as well as extrema count are provided in Table 1. This information provides a general quantitative outline of the computation process. We like to remind again that when only cubic interpolation is used, the process does not converge.

We used a Lenovo™ IdeaPad 130-15IKB laptop with an Intel® Core™ i5-8250 CPU and 20 GB of RAM to derive the processing times in Table 1. They may vary between different computers, development environments and code structure. We can see that the biharmonic spline interpolation for component #5 takes a considerable amount of time, but afterwards the number of extrema quickly goes to 1. Building envelope surfaces using cubic interpolation is quite fast and helps reduce the minima and maxima count so that we can use the biharmonic spline method.

Table 1

Processing time and number of extrema for each EMD component calculation

Interpolation method	Component #	Number of extrema	Processing time [s]
Cubic	1	167.01E+04	23.51
Cubic	2	28.91E+04	13.08
Cubic	3	9.14E+04	11.32
Cubic	4	4.70E+04	10.61
Biharmonic spline	5	3.94E+04	5395.45
Biharmonic spline	6	0.33E+04	423.66
Biharmonic spline	7	424	56.67
Biharmonic spline	8	44	7.41
Biharmonic spline	9	1	0.92

4. RESULTS

After having found a robust way of decomposing an image into its empirical mode components, we investigated how to manipulate them to achieve noise reduction after reconstruction. Firstly, we examined and reconstructed the hologram from each component individually. For different recorded objects all the relevant information was contained in the first two decompositions. The first component contained most useful image information, the second one contained some lower frequency image information, and components 3–9 had other low-frequency signals and the DC-term. This result, regarding the distribution of low and high-frequency data throughout the decomposition components, matches previous findings [5]. The reconstructions of the components can be seen in Figure 3.

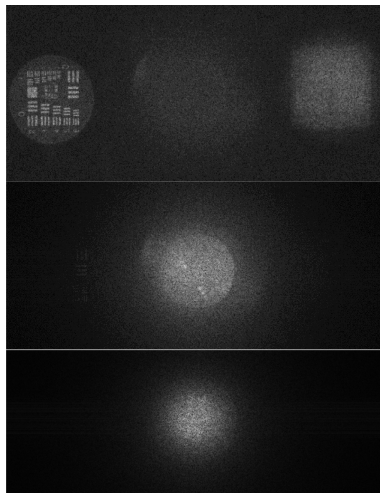
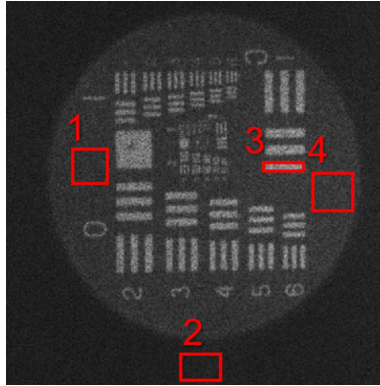


Figure 3. The first, second and third component reconstructions. White stripes in the second image are visible to the right of the DC-term

Figure 4. Areas for which V is calculated

This result pointed us to reconstructing the sum of the first two components only and examining the normalized contrast for the areas specified in Figure 4.

Finally, the contrast values for the filtered hologram are compared with the results from a standard Fresnel reconstruction where the hologram is not filtered. A slight but consistent improvement is present, which can be seen in Table 2.

Table 2

Contrast values for the different regions

V	Unfiltered	2D-HHT
Region 1	0.5201	0.5191
Region 2	0.5388	0.5378
Region 3	0.5299	0.5296
Region 4	0.5219	0.5212

We also tried adding additional noise components to the sum closely related to the specific speckle pattern. We tried adding different speckle patterns to various components, removing only selected ones, and adding multiple speckle patterns. However, these manipulations were not beneficial to noise reduction. We also tried a new decomposition of the sum of the first and last components, but it did not produce any significant change. With that, we have concluded that for holograms made with the setup shown in Figure 1, the best application of the 2D-HHT is to select only the first two components and discard the rest. Throughout the rest of the paper, we are going to use only the first two components from the empiric mode decomposition.

Further examination of the method shows its beneficial effect in reducing the zeroth order image (also known as the DC-term). It is a result of the imaging equations and off-axis holographic setup [18]. The DC-term appears as a very bright spot at the center of the reconstructed image and is of no practical use. Although more efficient methods [16] exist for its removal, the effect is considerable and should

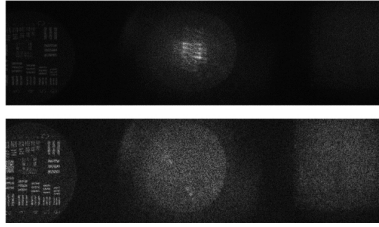


Figure 5. Top – nontreated hologram, bottom – hologram after application of the 2D-HHT algorithm. The images on the bottom are clearer as the bright DC-term is removed

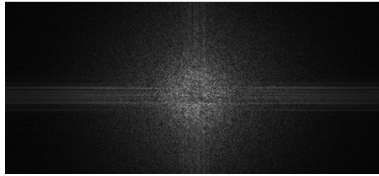


Figure 6. The sum of the seven unwanted HHT components

be mentioned. It can be observed in Figure 5. The sum of the seven discarded components can also be reconstructed and viewed. It consists of parts of the DC-term and background noise and lacks any information about the object. It was calculated that this sum of components has a mean value of 5% of the mean value of the untreated image, meaning that with its removal, 5% of the unwanted signal was discarded. The sum can be observed in Figure 6.

All these discoveries confirm our hypothesis that part of the unwanted signal or noise is contained in the decomposition components, and by discarding them, noise reduction is achieved. It means that 2D-HHT is a viable method for hologram filtering.

An investigation into the smallest resolvable details in both restored images shows no loss of spatial resolution when applying the 2D-HHT algorithm to a hologram (Figure 7).

5. FURTHER INVESTIGATION

2D-HHT can operate successfully on recorded holograms without a change in resolution so it can be combined with existing noise-filtering methods.

Here we have used 2D-HHT in combination with the Frost filter [11], BM3D [3, 4, 7] and NLM [32, 34] methods. We have chosen these techniques due to their performance and straight-forward application. The NLM filter was set up for a search window size of 11 pixels and a comparison window size of 5 pixels. BM3D was run with default parameters. The Frost filter had a damping parameter of 0.7 and a search window of 5 pixels. We evaluated the noise suppression at three spots in the reconstructed hologram – two inside and one outside the recorded object. It

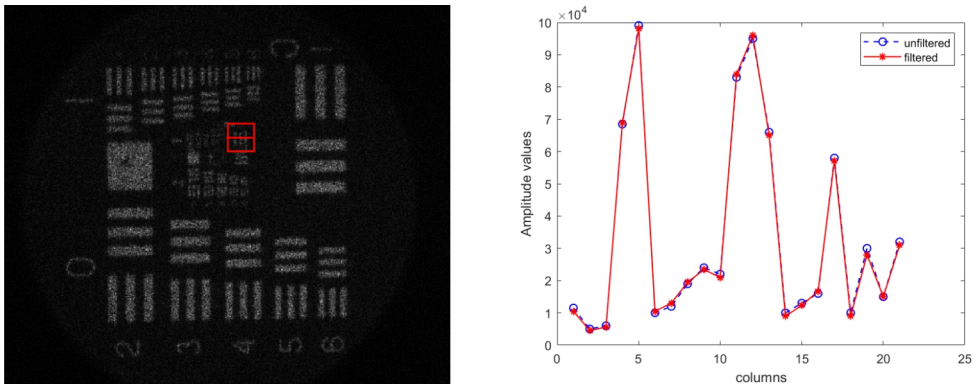


Figure 7. Inspection of the resolution. Left – selection of the finest detail to evaluate, right – a cross-section of the three white stripes, circles – 2D-HHT, stars – unfiltered

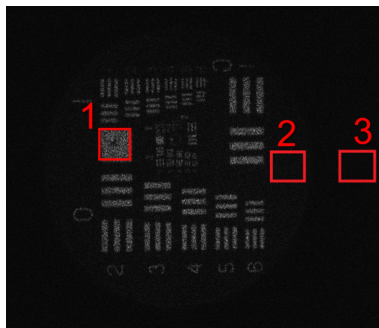


Figure 8. Regions for contrast estimation

gives us a good overview of the overall filtering performance. The spots are shown in Figure 8.

The contrasts for those areas are calculated and presented in Figures 9, 10 and 11.

Figures 9–11 show how contrast is affected when our method is applied to existing filtering techniques. For all areas of interest, an additional noise reduction can be observed for the holograms treated with the 2D-HHT algorithm.

An additional check into the method’s usefulness was carried out on simulated holograms. Instead of a conventionally recorded hologram, we generated an interference pattern by a GPU algorithm [30] without adding thermal noise. It was done to show that the current method not only deals with camera noise but also has an overall beneficial effect on the hologram. Contrast values for several areas were calculated and displayed in Table 3.

Using a computer simulated hologram allowed us to measure the MSE value (Eq. (3.2)). Results for different speckle sizes are presented in Figure 13.

Similarly, a small but consistent improvement in the MSE values can be observed for the filtered hologram.

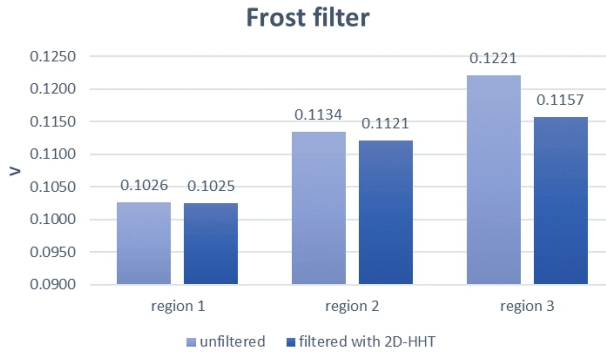


Figure 9. Contrast estimation for the Frost filter. The normalized contrast in on the y -axis. The blue bars on the left show results for application of the Frost filter only, while the orange bars to the right combine our method and the Frost filter

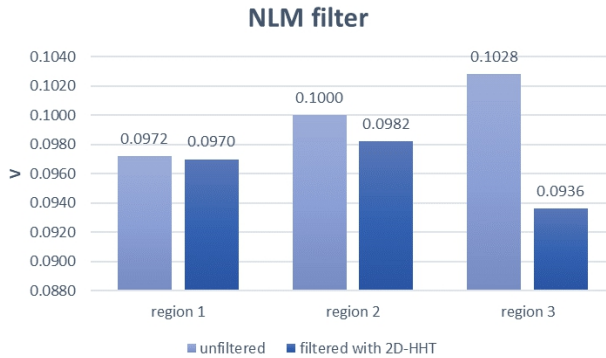


Figure 10. Contrast estimation for the NLM filter. The normalized contrast in on the y -axis. The blue bars on the left show results for application of the NLM filter only, while the orange bars to the right combine our method and the NLM filter

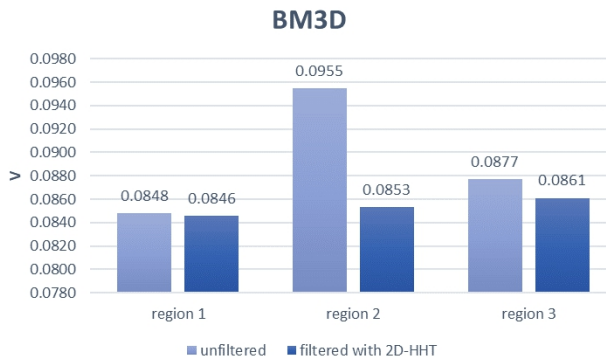


Figure 11. Contrast estimation for the BM3D filter. The normalized contrast in on the y -axis. The blue bars on the left show results for application of the BM3D filter only, while the orange bars to the right combine our method and the BM3D filter

Table 3

Contrast estimation for simulated hologram

V	Unfiltered	2D-HHT
Region 1	0.3603	0.3601
Region 2	0.5277	0.5214
Region 3	0.3706	0.3704



Figure 12. Contrast estimation areas on the simulated hologram

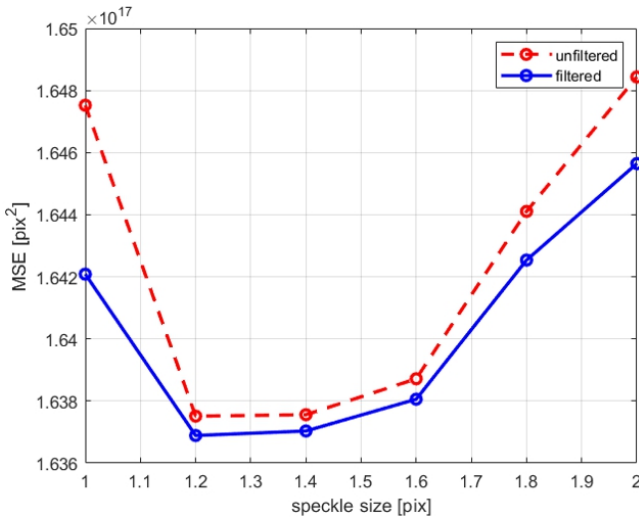


Figure 13. MSE value for different speckle sizes. The curve for the filtered holograms by our method is entirely below the curve for the untreated

6. CONCLUSION

This paper presented a novel method for noise reduction in digital holograms. It is based on the Hilbert-Huang transform and, unlike existing approaches, tackles the noise problem in the hologram plane. Various beneficial effects of the method were demonstrated, including reduced normalized contrast, DC-term removal and background noise reduction. Furthermore, the technique preserves image resolution, which allows it to be combined with other existing methods. A detailed evaluation of the noise reduction has been carried out. The proposed method was found to keep its beneficial effects when combined with existing techniques. It helps to further reduce the normalized contrast without impact on resolution. Future developments of the method include investigation of parallelization of different parts of the tech-

nique, such as the scattered data interpolation algorithms. Calculating the envelope surfaces on a GPU could help reduce processing times.

ACKNOWLEDGEMENTS

The result presented in this paper is part of the GATE project.

The GATE project has received funding from the European Union's Horizon 2020 WIDESPREAD-2018-2020 TEAMING Phase 2 programme under Grant Agreement No. 857155 and Operational Programme Science and Education for Smart Growth under Grant Agreement No. BG05M2OP001-1.003-0002-C01.

REFERENCES

- [1] P. Alfeld, Scattered data interpolation in three or more variables, in: *Mathematical methods in computer aided geometric design*, Elsevier, 1989, 1–33.
- [2] V. Bianco et al., Random resampling masks: a non-Bayesian one-shot strategy for noise reduction in digital holography, *Opt. Lett.* 38(5) (2013) 619–621.
- [3] V. Bianco et al., Quasi noise-free digital holography, *Light Sci. Appl.* 5 (2016) e16142.
- [4] V. Bianco et al., Strategies for reducing speckle noise in digital holography, *Light: Sci. Appl.* 7(1) (2018) 48.
- [5] A.-O. Boudraa and J.-C. Cexus, EMD-based signal filtering, *IEEE Trans. Instrum. Meas.* 56(6) (2007) 2196–2202.
- [6] W. Chen, B. Javidi and X. Chen, Advances in optical security systems, *Adv. Opt. Photonics* 6(2) (2014) 120–155.
- [7] K. Dabov et al., Image denoising by sparse 3-D transform-domain collaborative filtering, *IEEE Trans. Image Process* 16(8) (2007) 2080–2095.
- [8] K. Dabov et al., Image restoration by sparse 3D transform-domain collaborative filtering, in: *Image Processing: Algorithms and Systems VI*, SPIE, 2008.
- [9] R. Erf, *Holographic nondestructive testing*, Elsevier, 2012.
- [10] R. Franke and G. M. Nielson, Scattered data interpolation and applications: A tutorial and survey, in: *Geometric Modeling*, ed. by H. Hagen and D. Roller, *Computer Graphics – Systems and Applications*, Springer, Berlin, Heidelberg, 1991, 131–160.
- [11] V. Frost et al., An adaptive filter for smoothing noisy radar images, *Proc. IEEE* 69(1) (1981) 133–135.
- [12] R. Grant and G. Brown, Holographic nondestructive testing (HNDT) in the Automotive Industry, *SAE Transactions* 78 (1969) 305–313.
- [13] H. Jiang, J. Zhao and J. Di, Digital color holographic recording and reconstruction using synthetic aperture and multiple reference waves, *Opt. Commun.* 285(13–14) (2012) 3046–3049.
- [14] M. K. Kim, Digital holographic microscopy, in: *Digital Holographic Microscopy*, Springer, 2011, 149–190.
- [15] K. Kosma et al., Digital holographic interferometry for cultural heritage structural diagnostics: A coherent and a low-coherence optical set-up for the study of a marquetry sample, *Strain* 54(3) (2018) e12263.
- [16] T. Kreis, *Handbook of holographic interferometry: optical and digital methods*, John Wiley & Sons, 2006.
- [17] Y. Kuratomi et al., Speckle reduction mechanism in laser rear projection displays using a small moving diffuser, *JOSA A* 27(8) (2010) 1812–1817.

- [18] E. N. Leith and J. Upatnieks, Holograms: their properties and uses, *Opt. Eng.* 4(1) (1965) 3–6.
- [19] Y.-W. Liu, Hilbert transform and applications, in: *Fourier Transform Applications*, ed. by S. M. Salih, 2012, 291–300, <https://doi.org/10.5772/37727>.
- [20] E. Quak and L. L. Schumaker, Cubic spline fitting using data dependent triangulations, *Comput. Aided Geom. Des.* 7(1–4) (1990) 293–301.
- [21] N. Rehman and D. P. Mandic, Multivariate empirical mode decomposition, *Proc. R. Soc. A: Math. Phys. Eng. Sci.* 466(2117) (2010) 1291–1302.
- [22] G. Rilling, P. Flandrin and P. Goncalves, On empirical mode decomposition and its algorithms, in: *IEEE-EURASIP Workshop on Nonlinear Signal and Image Processing*, IEEEER Grado, 2003.
- [23] L. Rong et al., Speckle noise reduction in digital holography by use of multiple polarization holograms, *Chin. Opt. Lett.* 8(7) (2010) 653–655.
- [24] J. Rosen and G. Brooker, Fluorescence incoherent color holography. *Opt. Express* 15(5) (2007) 2244–2250.
- [25] O. Rukundo and H. Cao, Nearest neighbor value interpolation, arXiv preprint arXiv:1211.1768, 2012.
- [26] D. T. Sandwell, Biharmonic spline interpolation of GEOS-3 and SEASAT altimeter data, *Geophys. Res. Lett.* 14(2) (1987) 139–142.
- [27] J. Schmitt et al., 2D Hilbert-Huang transform, in: *2014 IEEE Int. Conf. on Acoustics, Speech and Signal Processing (ICASSP)*, IEEE, 2014.
- [28] U. Schnars and W. Jüptner, Direct recording of holograms by a CCD target and numerical reconstruction, *Appl. Opt.* 33(2) (1994) 179–181.
- [29] D. Shepard, A two-dimensional interpolation function for irregularly-spaced data, in: *Proc. 1968 23rd ACM National Conf.*, 1968.
- [30] T. Shimobaba et al., Fast calculation of computer-generated-hologram on AMD HD5000 series GPU and OpenCL, *Opt. Express* 18(10) (2010) 9955–9960.
- [31] V. Tornari et al., Impact of relative humidity on wood sample: A climate chamber experimental simulation monitored by digital holographic speckle pattern interferometry, *J. Imaging* 5(7) (2019) 65.
- [32] A. Uzan, Y. Rivenson and A. Stern, Speckle denoising in digital holography by non-local means filtering, *Appl. Opt.* 52(1) (2013) A195–A200.
- [33] R. F. Vanligten and H. Osterberg, Holographic microscopy, *Nature* 211(5046) (1966) 282–283.
- [34] J. Xiao et al., Nonlocal means filter based on cosine similarity applied in speckle reduction of digital holography, *Appl. Opt.* 61(25) (2022) 7474–7481.
- [35] F. Yaraş, H. Kang and L. Onural, State of the art in holographic displays: a survey, *J. Disp. Technol.* 6(10) (2010) 443–454.
- [36] T. Zeng, Y. Zhu and E. Y. Lam, Deep learning for digital holography: a review, *Opt. Express* 29(24) (2021) 40572–40593.

Received on April 9, 2024

Revised on May 21, 2024

Accepted on May 31, 2024

SIMEON KARPUZOV AND GEORGE PETKOV

Sofia University "St. Kliment Ohridski", GATE Institute
5, James Bourchier Blvd
1164 Sofia
BULGARIA

E-mails: simeon.karpuzov@gate-ai.eu
georgi.petkov@gate-ai.eu

ASSEN SHULEV

Institute of Mechanics, Bulgarian Academy of Sciences
Acad. G. Bontchev St., Bl. 4
1113 Sofia
BULGARIA

E-mail: assen@imbm.bas.bg